A Novel Methodological Approach to assessing Deformation and Force in Barrette Walls using FEM and ANOVA

Luan Nhat Vo
Faculty of Engineering and Technology, Van Hien University, Ho Chi Minh City, Vietnam
luanvn@vhu.edu.vn

Truong Xuan Dang
Ho Chi Minh University of Natural Resources and Environment, Ho Chi Minh City, Vietnam
dxtruong@hcmunre.edu.vn

Phuong Tuan Nguyen
Mien Tay Construction University, Vinh Long Province, Vietnam
tuanphuongvk@gmail.com

Hoa Van Vu Tran
The SDCT Research Group, University of Transport Ho Chi Minh City, Ho Chi Minh City, Vietnam
hoa.tranvu.htgroup@gmail.com

Tuan Anh Nguyen
University of Transport, Ho Chi Minh City, Vietnam
tuanna@ut.edu.vn (corresponding author)

Received: 30 May 2024 | Revised: 13 July 2024 | Accepted: 19 July 2024

Licensed under a CC-BY 4.0 license | Copyright (c) by the authors | *DOI: https://doi.org/10.48084/etasr.7975*

ABSTRACT

This research advances the understanding of deep excavation impacts by integrating a refined Finite Element Method (FEM) analysis with empirical data, specifically examining the behavior of retaining structures in urban environments. Unlike prior studies that predominantly relied on theoretical models, this paper combines FEM with statistical methods, particularly ANOVA, to identify critical factors affecting the performance of barrette walls during excavation. The primary objective of this study is to analyze the deformation and force behaviors at various depths, thereby enhancing the predictive capabilities of existing models. The findings highlight significant variations in horizontal displacements (U_y) and vertical displacements (U_z) across different excavation stages, with notable mean differences ranging from 0.000529420 m to 0.000700240 m for U_y and -0.017563652 m for U_z. Axial forces (N_1) also show significant increases with depth, reaching a mean difference of 516.137991 kN/m. These results underscore the importance of adaptive design strategies in deep excavation projects. However, the study is limited by the specific geological conditions and the scope of empirical data used for model validation. Practical recommendations include enhancing real-time monitoring systems and applying refined methodologies.

Keywords-barrette walls; deep excavation; FEM; ANOVA tests; deformation

I. INTRODUCTION

The construction of deep excavations in urban environments necessitates a profound understanding of the deformation behaviors and forces acting on retaining walls to ensure structural safety and prevent potential failures [1-5]. The significance of this research is underscored by the increasing demands of urban infrastructure projects, which often push the boundaries of construction into challenging geotechnical conditions [6, 7]. Deep excavations can induce significant deformations and internal forces within retaining structures, posing substantial risks to both the excavation site and adjacent

structures [8-10]. Therefore, it is crucial to develop comprehensive models and strategies to predict and control these deformations. Previous studies have highlighted various geotechnical factors influencing the performance of earth retaining walls during deep excavations. For instance, authors in [11] emphasized the importance of dynamic deformation control and real-time monitoring in managing excavation-induced risks. Similarly, authors in [12] analyzed the deformation of existing structures near deep excavations, demonstrating the critical role of monitoring horizontal and vertical displacements to ensure stability. Also authors in [13, 14] investigated deformation behaviors in soft soil areas, showing that axial forces and lateral displacements significantly increase with excavation depth, necessitating adaptive design strategies. Despite these advances, there remains a need for more refined analytical approaches that integrate empirical data with advanced modeling techniques. This study addresses this gap by combining Finite Element Method (FEM) analysis with statistical methods, specifically ANOVA testing, to identify critical factors affecting the performance of barrette walls during deep excavations. This integrated approach provides a detailed understanding of how different stages of excavation impact the stability and integrity of retaining structures, offering a significant advancement over previous models that predominantly relied on theoretical assumptions.

The contributions of this research to the field of geotechnical engineering are both theoretical and practical. Theoretically, it enhances the understanding of deformation dynamics and structural forces in deep excavations, supporting the development of more robust geotechnical models. Practically, it offers insights into improving design and construction practices for retaining structures, thereby enhancing safety and efficiency in urban infrastructure projects. By addressing the complexities of soil-structure interactions and the varying conditions encountered during deep excavations, this study provides valuable guidelines for engineers in the field.

II. MATERIALS AND METHODS

The excavation site under study is characterized by a geological setup that includes two primary soil layers: the upper layer which consists of mixed clay and extending down to 7.5 m, and the underlain sandy soil layer that continues to a depth of 32.5 m [15, 16]. Table I shows the soil parameters. The excavation area, adjacent to a single-story building, spans 11 m by 44 m, with a targeted excavation depth of 15 m [17, 18]. For optimal access and efficiency, excavation activities commence from both ends of the site (Figure 1) and are divided into 6 layers (Table II).

To ensure the stability of the excavation walls (Table III) and to prevent structural failures, a sophisticated shoring system is implemented, comprising four layers positioned at depths of -1 m, -4.6 m, -7.1 m, and -9.6 m [19]. This system is reinforced with H-beam steel sections measuring 400 × 400 mm (Table IV), which is essential for maintaining the structural integrity of the excavation walls [18, 20].

TABLE I. SOIL DESCRIPTION PARAMETERS WITH HARDENING SOIL MODEL

Parameter	Soil Type	
	Clay	Sand
Soil Model	Hardening Soil	Hardening Soil
Drainage Type	Undrained	Undrained
γ_w (kN/m^3)	20.25	20.12
γ_{sat}	20.57	20.55
e_{init}	0.5879	0.5810
n_{init}	0.3702	0.3675
E_{50}^{ref}	6875	13.45E3
E_{ode}^{ref}	6875	1345E3
E_{ur}^{ref}	20.63E3	40.35E3
V_{ur}	0.2	0.2
Power (m)	0.8	0.65
P^{ref}	38	400
C'^{ref}	7.1	5.7
φ' (°)	30.40	30
Ψ (°)	0.4	0
K_Z (m/day)	1.43E-05	6.91E-6
$K_X=K_y$	3.59E-05	0.138E-3

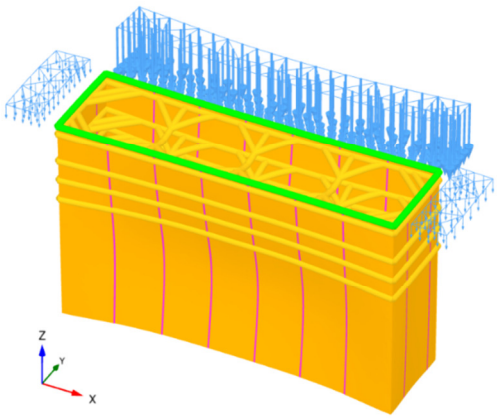

Fig. 1. Model of deep-dug pits.

TABLE II. ALTITUDE OF EXCAVATED SOIL LAYERS

No	The soil layer	Altitude (m)
1	Layer 1	0 – (-2)
2	Layer 2	(-2) – (-5.1)
3	Layer 3	(-5.1) – (-7.6)
4	Layer 4	(-7.6) – (-10.1)
5	Layer 5	(-10.1) – (-13.1)
6	Layer 6	(-13.1) – (-15.0)

Above these walls, a cap beam (Table V) with dimensions of 800×800 mm is installed to connect the barrette walls, enhancing the overall stability of the structure [21, 22]. The process begins with the installation of the cap beam, which provides essential lateral support and serves as the foundation for subsequent excavation and shoring activities. As the excavation deepens, each additional layer of the shoring system

is strategically added to provide temporary support, effectively preventing the collapse of the excavation walls.

TABLE III. BARRETTE WALL PARAMETERS

Parameter	Barrette Walls
Material Type	**Elastic**
Y (kN/m^3)	8
E1 (kN/m^2)	32.50E6
E2 (kN/m^2)	32.50E6
D (m)	0.8
G12 (kN/m^2)	16.25E6
G13 (kN/m^2)	16.25E6
G23 (kN/m^2)	16.25E6

TABLE IV. PARAMETERS DESCRIBING SHORING SYSTEM MATERIALS

Parameter	Value
Material Type	**Elastic**
Y (kN/m^3)	78.5
A (m^2)	0.02187
I2 (m^4)	0.666E-3
I3 (m^4)	0.224E-3
E (kN/m^2)	210.0E6

TABLE V. CAP BEAM MATERIAL DESCRIPTION PARAMETERS

Parameter	Value
Material Type	**Elastic**
Y (kN/m^3)	25
Height (m)	0.8
Width (m)	0.8
A (m^2)	0.02187
I2 (m^4)	0.666E-3
I3 (m^4)	0.224E-3
E (kN/m^2)	210.0E6

The presence of groundwater at a depth of -4 m introduces additional complexity to the excavation process. Managing the groundwater table is crucial. It is methodically lowered to counteract hydrostatic pressure, thus mitigating the risk of destabilizing water inflow [23]. This detailed approach ensures controlled and safe progression of the excavation toward the desired depth. The research model utilized in this study integrates the FEM with statistical analysis, specifically ANOVA testing, to investigate the deformation behaviors and forces acting on barrette walls during deep excavations. The FEM model represents both the geometry and material properties of the barrette walls and the surrounding soil, allowing for the simulation of the excavation process and analysis of structural responses under various loading and environmental conditions. This approach addresses the need to understand the complex interactions between soil and retaining structures, which are critical for predicting and controlling deformations. The study site comprises a geological setup with clay and sandy soil layers, with a targeted excavation depth of 15 m. The excavation process is systematically divided into 6 layers to assess the deformation and forces at different depths. Statistical analysis, particularly ANOVA, is employed to identify significant differences in technical parameters across various excavation stages, thereby pinpointing the critical factors that must be considered in the design and construction phases.

Initially, Levene's test was conducted to evaluate the homogeneity of variances among the groups. When the significance value (Sig. < 0.05) indicated non-homogeneous variances across all variables, it necessitated the use of the Welch ANOVA method instead of traditional ANOVA (Figure 2) [24]. The Welch ANOVA revealed statistically significant differences with Sig. < 0.05 for the variables analyzed. To gain a deeper understanding of the specific differences between variables, the Games-Howell post-hoc test was applied (Sig < 0.05) [25].

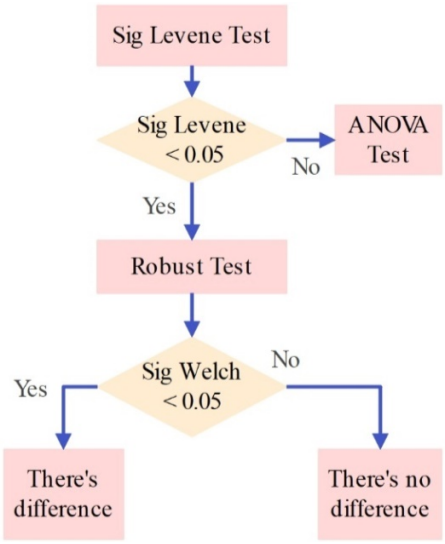

Fig. 2. Levene test procedure when Sig Levene < 0.05.

This integrated methodology not only refines existing theoretical models, but also provides practical guidelines for enhancing the stability and safety of deep excavation projects.

III. RESULTS

The deformation analysis across the 6 layers reveals a progressive increase in both maximum and minimum deformation values with depth (Table VI). Specifically, the maximum horizontal U_X, U_y, and vertical U_Z deformations show a trend where deeper layers exhibit greater deformation.

TABLE VI. DEFORMATION RESULTS OF BARRETTE WALLS DURING CONSTRUCTION

Layer		U_X (m)	U_Y (m)	U_Z (m)	$\|U\|$ (m)
Layer 1	Max	0.000639309	0.00460859	0.004541712	0.009376002
	Min	-0.000644046	-0.008204757	0.00390389	0.003907114
Layer 2	Max	0.001138263	0.012922488	0.011287489	0.019063729
	Min	-0.001149725	-0.015377348	0.010170291	0.010199781
Layer 3	Max	0.001280871	0.021150024	0.016075406	0.028139029
	Min	-0.001321378	-0.023192194	0.014566378	0.014588348
Layer 4	Max	0.001790015	0.028498884	0.019963685	0.036187305
	Min	-0.001841312	-0.030369791	0.018190714	0.018212335
Layer 5	Max	0.002523349	0.03811277	0.022807191	0.045778635
	Min	-0.002582716	-0.039977073	0.020816882	0.020839348
Layer 6	Max	0.002921124	0.048432929	0.023040189	0.055545013
	Min	-0.002987572	-0.050888014	0.020899777	0.020913295

For instance, the maximum total deformation $|U|$ escalates significantly from 0.009376002 m (Figure 3) in Layer 1 to 0.055545013 m (Figure 4) in Layer 6, indicating increased soil movement and instability with depth. Axial forces result from barrette walls during construction.

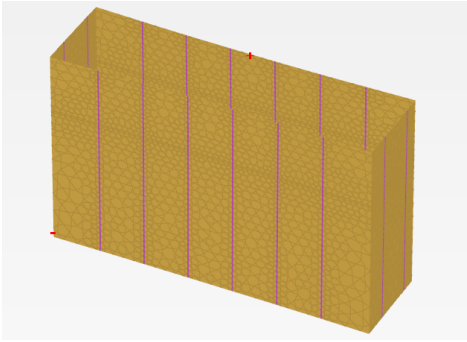

Fig. 3. Total displacements $|U|$ in Layer 1.

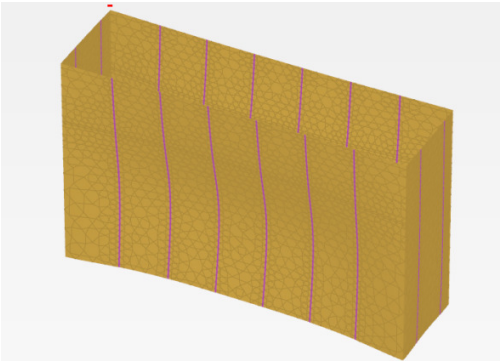

Fig. 4. Total displacements $|U|$ in Layer 6.

The analysis of axial forces across the 6 layers of the excavation site illustrates a complex interplay of forces, with both maximum (Figure 5) and minimum (Figure 6) values increasing substantially with depth.

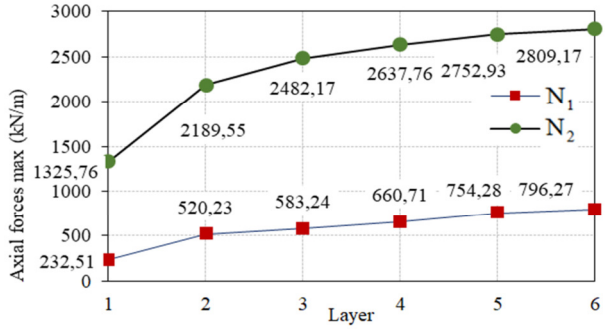

Fig. 5. The result max axial forces of N_1 and N_2 during excavation.

Notably, the maximum axial forces in N_1 and N_2 increase progressively from 232.51 kN/m and 1325.76 kN/m in Layer 1 to 796.27 kN/m and 2809.17 kN/m in Layer 6 (Table VII), respectively. This trend indicates a significant increase in load-bearing demands and potential structural stress in deeper layers. Conversely, the minimum values show a marked increase in negative force, from -270.68 kN/m in Layer 1 to -2019.69 kN/m in Layer 6 for N_1, suggesting an increase in tensile stresses or downward pulling forces, which are critical for maintaining excavation stability and preventing soil collapse. The analysis of shear forces across the 6 layers of the excavation site reveals a pattern of increasing magnitude in both the maximum (Figure 7) and minimum (Figure 8) shear forces as depth increases.

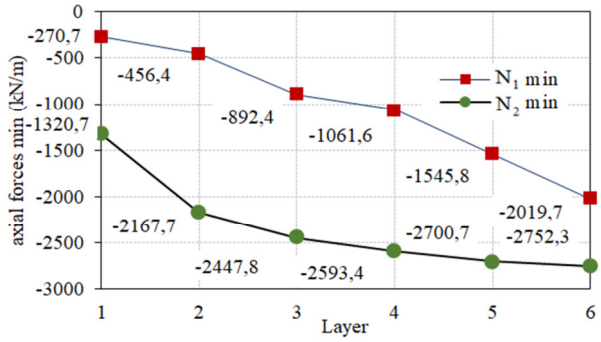

Fig. 6. The result min axial forces of N_1 and N_2 during excavation.

TABLE VII. AXIAL FORCES RESULT FROM BARRETTE WALLS DURING CONSTRUCTION

Layer	Value	N_1 (kN/m)	N_2 (kN/m)
Layer 1	Max	232.5086473	1325.7561
	Min	-270.6847398	-1320.717292
Layer 2	Max	520.2250267	2189.554771
	Min	-456.4073821	-2167.672703
Layer 3	Max	583.2413246	2482.170114
	Min	-892.4135221	-2447.796137
Layer 4	Max	660.7054207	2637.763436
	Min	-1061.589981	-2593.359521
Layer 5	Max	754.2789629	2752.931673
	Min	-1545.783058	-2700.72047
Layer 6	Max	796.2720037	2809.170879
	Min	-2019.687449	-2752.271789

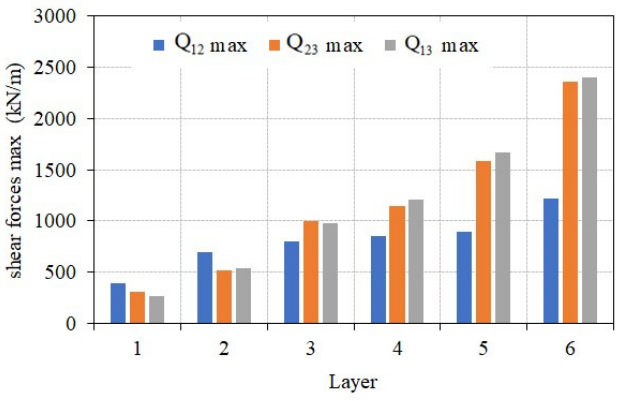

Fig. 7. The result max shear forces of Q_{12}, Q_{23}, and Q_{13} during excavation.

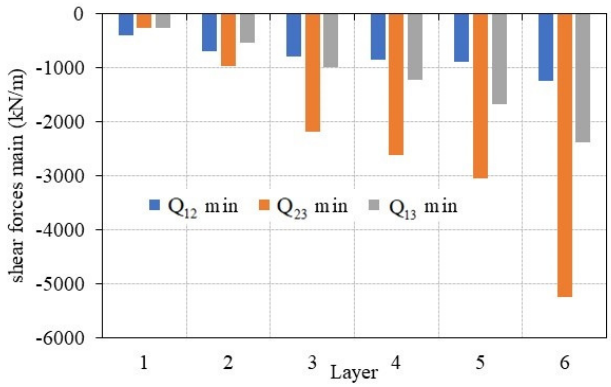

Fig. 8. The result min shear forces of Q_{12} , Q_{23} , and Q_{13} during excavation.

For instance, the shear forces in the Q_{12} , Q_{23} , and Q_{13} directions all exhibit significant growth from Layer 1 to Layer 6. The maximum values in Layer 1 are 389.43 kN/m, 307.50 kN/m, and 266.07 kN/m for Q_{12} , Q_{23} , and Q_{13} , respectively, escalating to 1220.21 kN/m, 2364.67 kN/m, and 2398.45 kN/m in Layer 6 (Table VIII).

TABLE VIII. SHEAR FORCES RESULTS OF BARRETTE WALLS DURING CONSTRUCTION

Layer	Value	Q_{12} (kN/m)	Q_{23} (kN/m)	Q_{13} (kN/m)
Layer 1	Max	389.4281959	307.4997199	266.0685461
	Min	-389.3392712	-258.4840556	-258.7400543
Layer 2	Max	695.1000519	512.4209406	540.675008
	Min	-694.4567908	-967.78315	-542.2370721
Layer 3	Max	797.6825955	993.356341	977.3608232
	Min	-796.6993098	-2178.523308	-976.9972789
Layer 4	Max	851.3978084	1143.13182	1211.162809
	Min	-849.9980603	-2622.980886	-1216.871175
Layer 5	Max	895.0316754	1588.218794	1668.110954
	Min	-891.6201713	-3053.128166	-1670.054314
Layer 6	Max	1220.210396	2364.668326	2398.450896
	Min	-1230.887923	-5251.199361	-2379.157017

This indicates a substantial increase in lateral and vertical stresses, reflecting greater soil movement and instability with increasing depth. The minimum values also demonstrate a significant deepening negative trend, suggesting increasing tensile stresses that can impact the structural integrity of the excavation site, particularly at deeper layers.

The bending moment analysis across the excavation site layers presents a progressive increase in both maximum and minimum bending moments with depth, indicating a rise in structural demands. Specifically, the maximum bending moments (Figure 9) in M_{11} increase from 101.45 kN m/m in Layer 1 to 731.70 kN m/m in Layer 6, while M_{22} increases from 108.70 kN m/m to 1389.80 kN m/m, suggesting greater lateral pressures and bending forces at deeper layers.

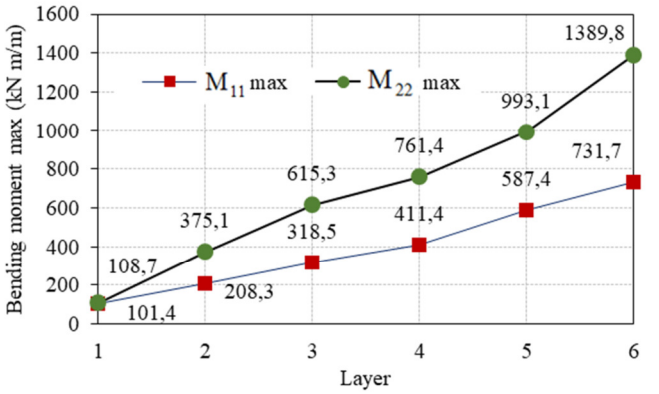

Fig. 9. The result max bending moment of M_{11} and M_{22} during excavation.

Conversely, the minimum values (Figure 10) also show a significant deepening negative trend, from -352.16 kN m/m in Layer 1 to -2349.47 kN m/m in Layer 6 for M_{11}, and from -106.68 kN m/m to -1341.28 kN m/m for M_{22} , reflecting increasing counteracting moments that could potentially influence the stability and design of retaining structures in deep excavation (Table IX).

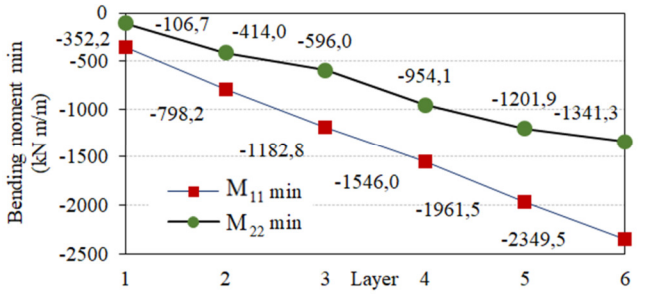

Fig. 10. The result bending moment min of M_{11} and M_{22} during excavation.

TABLE IX. BENDING MOMENT RESULTS OF BARRETTE WALLS DURING CONSTRUCTION

Layer		M_{11} (kN m/m)	M_{22} (kN m/m)
Layer 1	Max	101.4453288	108.7008665
	Min	-352.1602916	-106.6833113
Layer 2	Max	208.3461596	375.1440309
	Min	-798.1865373	-413.9501756
Layer 3	Max	318.4687064	615.3143427
	Min	-1182.843542	-596.0373381
Layer 4	Max	411.4494943	761.3741025
	Min	-1546.036173	-954.0534364
Layer 5	Max	587.4081304	993.0843384
	Min	-1961.509946	-1201.91431
Layer 6	Max	731.7029564	1389.798702
	Min	-2349.468063	-1341.276494

The torsion moment analysis across the 6 layers of the excavation site reveals a consistent pattern of increasing torsional stresses with depth. Specifically, the maximum torsion moments show a progressive increase from 105.75 kN m/m in Layer 1 to 617.38 kN m/m in Layer 6. Similarly, the

minimum values, indicative of counteracting torsional forces, also display a near-mirrored increase, from -105.15 kN m/m in Layer 1 to -617.85 kN m/m in Layer 6. This increasing trend underscores the growing torsional demands on the structural components as the excavation deepens, suggesting a need for enhanced structural reinforcements in deeper layers to manage these increasing torsional loads effectively (Table X).

The ANOVA results in Table XI detail the statistical analysis used to compare variances in the data, which aids in understanding the significant differences between groups.

The Test of Homogeneity of Variances reveals significant non-homogeneity across all variables, as indicated by the significance value (Sig.) of 0.000 for each. This uniformity in the results suggests substantial differences in variance among the groups being analyzed, necessitating the use of robust tests in subsequent analyses to accommodate these variances and ensure accurate interpretation of the data (Table XII).

TABLE X. MOMENT M_{12} RESULTS OF BARRETTE WALLS DURING CONSTRUCTION

Layer	Value	M_{12} (kN m/m)
Layer 1	Max	105.7461259
	Min	-105.153888
Layer 2	Max	218.4946393
	Min	-218.5530949
Layer 3	Max	367.5080876
	Min	-367.574181
Layer 4	Max	447.1856242
	Min	-447.27241
Layer 5	Max	489.2916127
	Min	-489.4980441
Layer 6	Max	617.37966
	Min	-617.8496238

TABLE XI. TEST OF HOMOGENEITY OF VARIANCES

		Levene Statistic	df1	df2	Sig.
U_X	Based on mean	9807,904	5	285258	0.000
U_Y	Based on mean	15684.228	5	285258	0.000
U_Z	Based on mean	21537.992	5	285258	0.000
U	Based on mean	37656.876	5	285258	0.000
N_1	Based on mean	34746.387	5	285258	0.000
N_2	Based on mean	6030.605	5	285258	0.000
Q_{12}	Based on mean	2923.281	5	285258	0.000
Q_{23}	Based on mean	7196.933	5	285258	0.000
Q_{13}	Based on mean	7328.347	5	285258	0.000
M_{11}	Based on mean	9142.355	5	285258	0.000
M_{22}	Based on mean	13976.997	5	285258	0.000
M_{12}	Based on mean	9964.039	5	285258	0.000

TABLE XII. ROBUST TESTS OF EQUALITY OF MEANS

		Statistic (Asymptotically F distributed)	df1	df2	Sig.
U_X	Welch	2.347	5	123951.030	0.039
U_Y	Welch	33.441	5	120437.037	0.000
U_Z	Welch	18722369.024	5	126575.733	0.000
U	Welch	378791.913	5	121647.401	0.000
N_1	Welch	66537.931	5	120784.968	0.000
N_2	Welch	6646.315	5	127354.771	0.000
Q_{12}	Welch	0.189	5	124301.362	0.967
Q_{23}	Welch	345.895	5	120516.868	0.000
Q_{13}	Welch	0.041	5	119433.492	0.999
M_{11}	Welch	637.318	5	121850.564	0.000
M_{22}	Welch	6664.109	5	116103.498	0.000
M_{12}	Welch	0.362	5	122236.506	0.875

For U_X, U_y, U_Z, U, N_1, N_2, Q_{23}, M_{11}, and M_{22} the low significance values (ranging from 0.000 to 0.039) are less than 0.05, so it is concluded that these variables are different. However, variables Q_{12}, Q_{13}, and M_{12} show high Sig. values 0.967, 0.999, and 0.875, respectively, indicating no substantial difference in means across the groups for these particular variables. To select the variable with the most clearly different values, perform a Games-Howell test is performed. The results of the Games-Howell analysis reveal that variable U_y shows particularly strong and consistent significant differences across nearly all comparisons between layers. The mean difference between layer 1 and layer 6 is 0.000700240 m (Sig. = 0.000), and between layer 1 and layer 5, it is 0.000529420 m (Sig. = 0.000). These significant values indicate that U_y changes substantially from one stage to another, reflecting major impacts due to changing conditions (Figure 11). Variable U_Z also shows significant changes across the layers. The mean difference between layer 1 and layer 6 is an extensive -0.017563652 m (Sig. = 0.000). Similarly, between layer 1 and layer 4, it is -0.014831164 m (Sig. = 0.000), demonstrating substantial variance, which points to significant shifts in conditions affecting this variable (Figure 11). Variable N_1 is another key influencer, with essential differences, such as between layer 1 and layer 6, where the mean difference reaches 516.137991 kN/m (Sig. = 0.000). This large magnitude in mean difference further emphasizes the impact of varying stages on N_1 (Figure 12).

Among the variables analyzed, U_y and U_Z stand out as being the most affected ones by the differences in stages, evidenced by their consistent and significant mean differences across multiple-stage comparisons. These variables showed the highest sensitivity to changes in stages, indicating their crucial role in the phenomena being studied. N_1 also shows significant sensitivity, though to a slightly lesser extent than U_y and U_Z. These findings suggest that U_y and U_Z should be closely

monitored and considered in further analyses and decision-making processes due to their crucial responses to changing experimental or operational conditions.

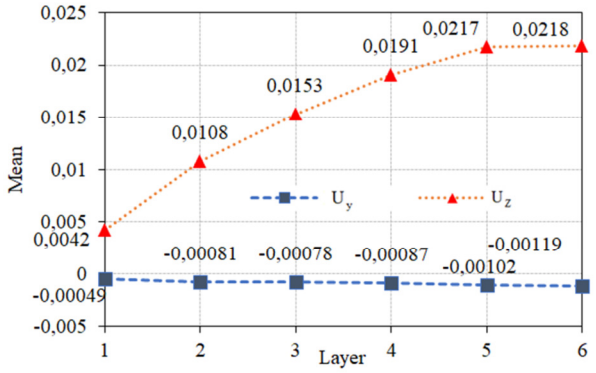

Fig. 11. The mean difference for U_y and U_Z between layer 1 and layer 6.

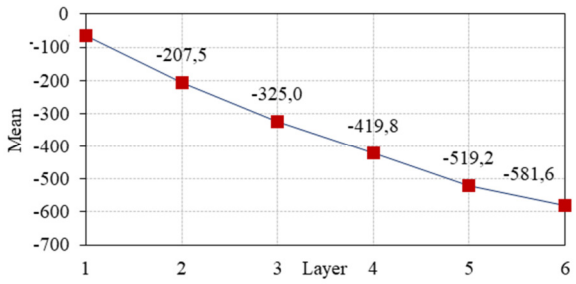

Fig. 12. The mean of N_1 between layer 1 and layer 6.

IV. DISCUSSION

The comprehensive analysis of deformation and force behaviors across various excavation stages offers pivotal insights into the intricate dynamics of deep excavation. Notably, variables U_y and U_Z demonstrated substantial variability across stages, underscoring their sensitivity to the differing geotechnical conditions encountered during excavation. U_y, in particular, exhibited consistent significant differences across stages, with the mean differences ranging from 0.000529420 m to 0.000700240 m (Sig. = 0.000), reflecting the impact of changing excavation depths and soil interactions. Similarly, U_Z presented marked changes with mean differences, such as -0.017563652 m between early and deeper stages (Sig. = 0.000), indicating the pronounced effect of soil stratification and the mechanical stresses involved. Moreover, the axial forces in N_1 highlighted an increasing trend with depth, with a notable difference of 516.137991 kN/m between the shallowest and deepest stages (Sig. = 0.000). This suggests a growing load-bearing demand and potential stress accumulation in the structure as the excavation deepens. These findings are crucial for improving the design and implementation of excavation projects, as they provide a quantified measure of how different stages of excavation can variably impact the stability and integrity of retaining structures.

The results from this study align with previous research in the field, such as the work in [11], which emphasized the importance of dynamic deformation control in retaining structures during deep excavations. Both studies highlight the necessity of real-time monitoring and adaptive design strategies to manage the risks associated with excavation-induced deformations. However, while authors in [11] focused on case-specific adjustments based on field monitoring data, the current study provides a broader analytical framework using FEM and ANOVA to understand deformation dynamics. Similarly, authors in [12] also underline the significance of vertical and horizontal displacement monitoring near deep excavations, particularly in urban settings with existing infrastructures like subway tunnels. Their findings on the interaction between enclosure structures and tunnel deformation support the observations in this study regarding the critical role of horizontal displacements U_y and vertical displacements U_Z.

In contrast, authors in [13, 14] provide detailed examinations of deformation behaviors in soft soil areas, demonstrating that axial forces and lateral displacements increase significantly with excavation depth. This is consistent with the current study's results, which also observed increased axial forces N_1 and substantial horizontal and vertical deformations with depth. A notable difference is the current study's detailed statistical analysis, which offers a more granular understanding of the variance and significance of these changes across different stages. These comparative insights affirm the broader applicability of the findings and underscore the importance of adaptive and real-time monitoring strategies in deep excavation projects to enhance safety and structural integrity.

V. CONCLUSIONS

This research highlights the critical influence of various excavation stages on the deformation and forces that impact the retention of structures in deep excavation environments. The results significantly underscore that variables such as horizontal displacements U_y and vertical displacements U_Z are crucial indicators of changes in the geotechnical properties as the excavation progresses deeper. For instance, the variations in U_y demonstrated considerable changes across stages, with significant mean differences ranging from 0.000529420 m to 0.000700240 m (Sig. = 0.000) between the initial and final stages. Similarly, U_Z showed substantial alterations, with a notable mean difference of -0.017563652 m (Sig. = 0.000) between early and deeper stages, reflecting the impact of increasing depth on structural behavior. Moreover, the increase in axial forces observed in N_1, with a significant mean difference of 516.137991 kN/m (Sig. = 0.000) between the uppermost and lowest layers, points to the increasing mechanical demands placed on the excavation as it deepens.

This study provides empirical evidence supporting the need for adaptive design strategies that account for the dynamic geotechnical conditions encountered during deep excavation

projects, thus contributing to safer and more efficient engineering practices. The novel contribution of this research lies in the integration of FEM analysis with advanced statistical methods, specifically ANOVA testing, to identify the critical factors that must be carefully considered during the design and construction phases of excavation. This combination offers a more rigorous and detailed understanding of how different stages of excavation impact the stability and integrity of retaining structures, providing a significant advancement over previous studies that relied predominantly on theoretical models.

The practical implications of this research are significant for the field of geotechnical engineering. By demonstrating how horizontal and vertical deformations vary with excavation depth, the findings offer critical insights for improving the design and implementation of retaining structures. The results can inform more accurate and adaptive design approaches, leading to enhanced stability and safety in urban excavation projects. Additionally, the refined methodologies for predicting deformation and ensuring structural integrity can be directly applied to optimize construction processes and mitigate risks associated with deep excavations.

The theoretical contributions of this study also advance the current knowledge in the field. The detailed statistical analysis, including the use of ANOVA, provides a granular understanding of the variance and significance of deformation changes across different excavation stages. This methodological enhancement contributes to a deeper theoretical understanding of the factors influencing structural behavior during deep excavations, thus supporting the development of more robust and reliable geotechnical models.

REFERENCES

[1] H. Zhu, L. Yao, and J. Li, "Influence factors on the seismic behavior and deformation modes of gravity retaining walls," *Journal of Mountain Science*, vol. 16, no. 1, pp. 168–178, Jan. 2019, https://doi.org/10.1007/s11629-018-5009-z.

[2] X. Chen, H. Guo, P. Zhao, X. Peng, and S. Wang, "Numerical modeling of large deformation and nonlinear frictional contact of excavation boundary of deep soft rock tunnel," *Journal of Rock Mechanics and Geotechnical Engineering*, vol. 3, pp. 421–428, Dec. 2011, https://doi.org/10.3724/SP.J.1235.2011.00421.

[3] S. Yasrebi and E. Zolqadr, "Numerical modelling for optimizing shoring wall performance in deep urban excavations," *IOP Conference Series: Earth and Environmental Science*, vol. 1336, no. 1, Feb. 2024, Art. no. 012004, https://doi.org/10.1088/1755-1315/1336/1/012004.

[4] Y. Han, Q. Xu, and Y. Cui, "Deformation of Existing Shield Tunnel Adjacent to Deep Excavations: Simulation and Monitoring Analysis," *Applied Sciences*, vol. 14, no. 10, Jan. 2024, Art. no. 4153, https://doi.org/10.3390/app14104153.

[5] V. S. S. D. Silva and L. I. N. de Silva, "Finite Element Analysis of a Deep Excavation supported using a Secant Pile Wall: A Case Study," in *2023 Moratuwa Engineering Research Conference (MERCon)*, Aug. 2023, pp. 521–526, https://doi.org/10.1109/MERCon60487.2023.10355502.

[6] C. J. Sainea-Vargas and M. C. Torres-Suárez, "Random Field-Based Numerical Modeling of Deep Excavation in Soft Soils for Adjacent Building Damage Probability Assessment," in *Challenges and Innovations in Geomechanics*, 2021, pp. 993–1000, https://doi.org/10.1007/978-3-030-64514-4_109.

[7] M. Zumrawi and A. El-Amin, "Importance of Deep Excavation Support and Its Influence on Adjacent Buildings," presented at the 7th Annual Conference for Postgraduate Studies and Scientific Research, Basic Sciences and Engineering Studies, University of Khartoum, Sudan, Mar. 2016.

[8] Q. X. Zhu, H. L. Qin, B. W. Song, L. Wang, and X. L. Lü, "A case study of the response of support structure and stratum deformation caused by deep foundation pit excavation in soft area," *IOP Conference Series: Earth and Environmental Science*, vol. 1336, no. 1, Feb. 2024, Art. no. 012024, https://doi.org/10.1088/1755-1315/1336/1/012024.

[9] D. Wang, S. Wang, Z. Zhang, and P. Ding, "Study of the Mechanical Behavior of Retaining Structures and Adjacent Buildings during the Excavation of Deep and Long Pits," *Shock and Vibration*, vol. 2024, no. 1, 2024, Art. no. 7242422, https://doi.org/10.1155/2024/7242422.

[10] W. Zhao *et al.*, "A numerical study on the influence of anchorage failure for a deep excavation retained by anchored pile walls," *Advances in Mechanical Engineering*, vol. 10, no. 2, Feb. 2018, Art. no. 1687814018756775, https://doi.org/10.1177/1687814018756775.

[11] C. Xu, Q. Chen, Y. Wang, W. Hu, and T. Fang, "Dynamic Deformation Control of Retaining Structures of a Deep Excavation," *Journal of Performance of Constructed Facilities*, vol. 30, no. 4, Aug. 2016, Art. no. 04015071, https://doi.org/10.1061/(ASCE)CF.1943-5509.0000819.

[12] J. Xie, Q. Xu, H. Yan, Y. Han, and L. Lu, "Mechanical performance and application of retaining structures doubling as permanent structures in deep excavations," *IOP Conference Series: Earth and Environmental Science*, vol. 1336, no. 1, Feb. 2024, Art. no. 012026, https://doi.org/10.1088/1755-1315/1336/1/012026.

[13] L. Shi, W. Yu, and L. Fu, "Deformation analysis of deep foundation pit in soft soil area considering space–time effect," *The Journal of Engineering*, vol. 2019, no. 11, pp. 8274–8281, 2019, https://doi.org/10.1049/joe.2018.5398.

[14] X. Liu and S. Liu, "Study on Deformation Characteristics of Deep Foundation Excavation in Soft-Soil and the Response of Different Retaining Configurations," *Geotechnical and Geological Engineering*, vol. 30, no. 2, pp. 313–329, Apr. 2012, https://doi.org/10.1007/s10706-011-9470-5.

[15] A. R. Leon Bal and G. Meschke, "Two-phase model for the excavation analysis in partially saturated soft soils using the particle finite element method," *International Journal for Numerical and Analytical Methods in Geomechanics*, vol. 47, no. 2, pp. 145–186, 2023, https://doi.org/10.1002/nag.3464.

[16] C.-Y. Chang and J. M. Duncan, "Analysis of Soil Movement Around a Deep Excavation," *Journal of the Soil Mechanics and Foundations Division*, vol. 96, no. 5, pp. 1655–1681, Sep. 1970, https://doi.org/10.1061/JSFEAQ.0001459.

[17] H. Li, Y. Tang, S. Liao, and M. Shen, "Structural Response and Preservation of Historic Buildings Adjacent to Oversized Deep Excavation," *Journal of Performance of Constructed Facilities*, vol. 35, no. 6, Dec. 2021, Art. no. 04021095, https://doi.org/10.1061/(ASCE)CF.1943-5509.0001676.

[18] X. He, S. Hu, L. Yang, Y. Chen, and X. Fu, "Three-dimensional numerical modelling of the effects of deep excavation on nearby buildings," in *International Conference on Electronic Information Engineering, Big Data, and Computer Technology (EIBDCT 2022)*, May 2022, Art. no. 12256, https://doi.org/10.1117/12.2635419.

[19] M. G. Freiseder and H. F. Schweiger, "Numerical Analysis of Deep Excavations," in *Application of Numerical Methods to Geotechnical Problems*, Vienna, 1998, pp. 283–292, https://doi.org/10.1007/978-3-7091-2512-0_27.

[20] F. Farrokhzad, S. MotahariTabari, H. Abdolghafoorkashani, and H. Tavakoli, "Seismic Behaviour of Excavations Reinforced with Soil–Nailing Method," *Geotechnical and Geological Engineering*, vol. 39, no. 6, pp. 4071–4091, Aug. 2021, https://doi.org/10.1007/s10706-020-01625-7.

[21] D.-W. Chang, D.-W. Huang, Y. K. Lin, F.-C. Lu, C.-J. Kuo, and A. Zhussupbekov, "Length Influences on Lateral Performance of Barrette from Three-Dimensional Finite Element Analysis," *Journal of Applied Science and Engineering*, vol. 25, no. 4, pp. 677–691, 2021, https://doi.org/10.6180/jase.202208_25(4).0003.

[22] J. Ye and M. Lu, "Optimization of domes against instability," *Steel and Composite Structures*, vol. 28, no. 4, pp. 427–438, Jan. 2018.

[23] Y.-X. Wu, H.-M. Lyu, S.-L. Shen, and A. Zhou, "A three-dimensional fluid-solid coupled numerical modeling of the barrier leakage below the excavation surface due to dewatering," *Hydrogeology Journal*, vol. 28, no. 4, pp. 1449–1463, Jun. 2020, https://doi.org/10.1007/s10040-020-02142-w.

[24] S. L. Braver, D. P. MacKinnon, and M. Page, *Levine's Guide to SPSS for Analysis of Variance*, 2nd ed. Mahwah, NJ, USA: Psychology Press, 2003.

[25] C. Mital and A. Rajyaguru, "Comparison of Post Hoc Tests for Unequal Variance," *International Journal of New Technologies in Science and Engineering*, vol. 02, no. 05, Nov. 2015.